Designing for beam propagation in periodic and nonperiodic photonic nanostructures: Extended Hamiltonian method

Yang Jiao, Shanhui Fan, and David A. B. Miller
Ginzton Laboratory, Stanford University, Stanford, California 94305-4088, USA
(Received 6 February 2004; published 23 September 2004)

We use Hamiltonian optics to design and analyze beam propagation in two-dimensional (2D) periodic structures with slowly varying nonuniformities. We extend a conventional Hamiltonian method, adding equations for calculating the width of a beam propagating in such structures, and quantify the range of validity of the extended Hamiltonian equations. For calculating the beam width, the equations are more than 10^3 times faster than finite difference time domain (FDTD) simulations. We perform FDTD simulations of beam propagation in large 2D periodic structures with slowly varying nonuniformities to validate our method. Beam path and beam width calculated using the extended Hamiltonian method show good agreement with FDTD simulations. By contrasting the method with ray tracing of the bundle of rays, we highlight and explain the limitations of the extended Hamiltonian method. Finally, we use a frequency demultiplexing device optimization example to demonstrate the potential applications of the method.

DOI: 10.1103/PhysRevE.70.036612 PACS number(s): 42.70.Qs, 42.15.Dp, 42.25.Dd, 61.50.Ah

I. INTRODUCTION

Radical dispersion properties of periodic photonic nanostructures [1,2] has recently generated much research interest [3]. For applications such as group velocity dispersion compensation and frequency demultiplexing, however, periodic structures arguably do not offer enough design freedom to achieve the desired input/output dispersion relation over large frequency ranges. In such cases, nonperiodic structures could perform much better than periodic structures [4,5]. Introducing nonuniformities in two-dimensional (2D) and three-dimensional (3D) periodic structures, such as high-index cylinder/sphere arrays, will also allow more freedom in the design of the device input/output characteristics. There has, however, been much less study of 2D and 3D nonuniform structures, partly due to the difficulty in analyzing them. Finite difference time domain (FDTD) simulations can be used to analyze such structures, but it is very time consuming [6]. In this work, we use a Hamiltonian optics method to design and analyze the beam path in for Gaussian beams propagating in 2D periodic structures with slowly varying nonuniformities. Furthermore, we extend the conventional Hamiltonian method with equations for calculating the beam width in periodic structures. For a beam propagating in a nonuniform structure, the extended Hamiltonian method can calculate the beam path and the beam width at least 10^3 times faster than FDTD simulations. Where slowness of the FDTD method restricts it to a tool for analyzing given structures, the speedup allows the extended Hamiltonian method to be used as a design tool for the intentional introduction of nonuniformities into periodic photonic structures for exciting device functions.

The efficiency of the extended Hamiltonian method relies on the local periodicity of the structure. If the nonuniformity occurs over many periods, locally the structure is approximately periodic. Therefore, we can define and calculate the Bloch wave dispersion relationship, locally, for each position inside the structure. With the dispersion relationship known, the classical optical Hamiltonian equations can be used to track the beam path for a ray propagating in the nonuniform structure. With the beam path known, we can then use the extended Hamiltonian equations that we developed to track the beam width for a Gaussian beam propagating in a nonuniform structure. The computational cost for calculating the dispersion relationship is amortized over all designs based on the same type of nonuniformities, e.g., all designs based on nonuniform distribution of the high index cylinder radius. After the dispersion relationships are calculated for each possible type of local structure, the speed advantage of the extended Hamiltonian method over FDTD is dramatic.

Previous work on applying Hamiltonian optics to periodic media solely dealt with the calculation of the ray path [7]. The classical Hamiltonian method is also useful for calculating the time of flight of a ray in nonuniform periodic media and the frequency dependency of the ray path [7]. The method has also been used to show that chaotic ray paths can be easily achieved in nonuniform periodic media [8]. However, without an understanding of the evolution of the beam width, practical design with such periodic media with nonuniformities would be very limited. For example, the beam width is critical for any beam steering device. Therefore, the beam width equation we introduce here is a critical refinement to the Hamiltonian method for analyzing propagation in periodic media with nonuniformities.

To the best of our knowledge, there are no previous published large-scale FDTD simulations of beam propagation in periodic media with gradual nonuniformity. In this work, we perform FDTD simulations of 2D periodic structures with nonuniformities, with dimensions on the order of 100×100 lattice constants. These simulations validate the beam path and the beam width calculated with the extended Hamiltonian equations. FDTD simulations of structures at this scale are very time consuming, whereas the computational complexity of the extended Hamiltonian equations is essentially independent of the device size.

In Sec. II we develop the extension to the Hamiltonian equations in the context of bulk media with slowly varying

nonuniformities. We explain the applicability of the extended Hamiltonian equations to periodic media with nonuniformities in Sec. III. In Sec. IV, we provide a measure for the range of validity of the extended Hamiltonian method, validate the method with FDTD simulations, and explain limitations of the method with a comparison to ray bundle tracing. Finally, we use a numerical optimization example in Sec. V to demonstrate the potential applications of the method.

II. THE HAMILTONIAN EQUATIONS AND EXTENSION

A. Hamiltonian optics

Hamiltonian optics has traditionally been used to describe the optical ray path in bulk dielectric media with slowly varying properties [9]. We will define the characteristic inhomogeneity length L as the shortest distance over which the nonuniformity changes the medium significantly. We assume the field behaves similar to a plane wave locally, and has the form $\mathbf{E}(\mathbf{x})=\mathbf{a}(\mathbf{x})\exp[is(\mathbf{x})]$, where $\mathbf{x}=\{x^1,x^2,x^3\}$ is a dimensionless coordinate system, scaled from real spatial coordinates $\{X^1,X^2,X^3\}$ as in $\{x^1,x^2,x^3\}=\{X^1/L,X^2/L,X^3/L\}$. By substituting the assumed form of $\mathbf{E}(\mathbf{x})$ into Maxwell's equations, and using the slowly varying approximation [e.g., the wave amplitude $\mathbf{a}(\mathbf{x})$ varies much more slowly than the phase, and therefore the spatial derivative of $\mathbf{a}(\mathbf{x})$ is ignored], we will get a equation for $\mathbf{a}(\mathbf{x})$:

$$\left[\left(\frac{c}{\omega}\right)^2(|\mathbf{k}|^2\mathbf{I}-\mathbf{k}\mathbf{k}^T)-\boldsymbol{\varepsilon}(\mathbf{x})\right]\mathbf{a}=0, \tag{1}$$

where ω is the frequency, $\boldsymbol{\varepsilon}(\mathbf{x})$ is the dielectric tensor, $\mathbf{I}$ is the identity matrix, we defined $\mathbf{k}=\nabla s$ as the wave vector, and $\mathbf{k}^T$ is the transpose of $\mathbf{k}$ (so that $\mathbf{k}\mathbf{k}^T$ forms a matrix or tensor). We assumed the nonuniformity comes from the spatial dependence of the dielectric tensor. Now we define the mathematical entity that will become the effective Hamiltonian for this problem, i.e., we choose

$$H(\mathbf{x},\mathbf{k},\omega)\equiv\det\left[\left(\frac{c}{\omega}\right)^2(|\mathbf{k}|^2\mathbf{I}-\mathbf{k}\mathbf{k}^T)-\boldsymbol{\varepsilon}(\mathbf{x})\right]. \tag{2}$$

In order for a nontrivial solution to exist for $\mathbf{a}$, we must have

$$\det\left[\left(\frac{c}{\omega}\right)^2(|\mathbf{k}|^2\mathbf{I}-\mathbf{k}\mathbf{k}^T)-\boldsymbol{\varepsilon}(\mathbf{x})\right]\equiv H(\mathbf{x},\mathbf{k},\omega)=0. \tag{3}$$

For fixed ω, we look for the parameterized curve $\{\mathbf{r}(\tau),\mathbf{q}(\tau)\}$ in the 6D space $\{\mathbf{x},\mathbf{k}\}$ such that Eq. (3) is satisfied. Here τ is the parameterization variable. If Eq. (3) is satisfied, then $\mathbf{r}(\tau)$ describes the path followed by the wave, and $\mathbf{q}(\tau)$ describes the wave vector along the path. We can now find that Eq. (3) is satisfied on the curve $\{\mathbf{r}(\tau),\mathbf{q}(\tau)\}$ if the curve obeys the Hamiltonian equations

$$\frac{d\mathbf{r}}{d\tau}=\frac{\partial H(\mathbf{x},\mathbf{k},\omega)}{\partial\mathbf{k}},\quad \frac{d\mathbf{q}}{d\tau}=-\frac{\partial H(\mathbf{x},\mathbf{k},\omega)}{\partial\mathbf{x}}. \tag{4}$$

It can be verified that Eq. (4) is a solution of Eq. (3) by taking the full derivative of the left-hand side of Eq. (3) with respect to τ, and substituting Eq. (4) into the expression, therefore justifying our choice for the effective Hamiltonian of the problem.

The widely used dispersion relationship $\omega(\mathbf{k},\mathbf{x})$ is obtained by solving Eq. (3) for fixed $\mathbf{x}$. We can write Eq. (4) in terms of the $\omega(\mathbf{x},\mathbf{k})$ rather than $H(\mathbf{x},\mathbf{k},\omega)$. Using the fact that, for a solution we must have $H(\mathbf{x},\mathbf{k},\omega(\mathbf{x},\mathbf{k}))=0$, and taking partial derivatives of $H(\mathbf{x},\mathbf{k},\omega(\mathbf{x},\mathbf{k}))$ with respect to $\mathbf{x}$ and $\mathbf{k}$, we get

$$\frac{\partial\omega}{\partial\mathbf{x}}=C(\mathbf{x},\mathbf{k})\frac{\partial H}{\partial\mathbf{x}},\quad \frac{\partial\omega}{\partial\mathbf{k}}=C(\mathbf{x},\mathbf{k})\frac{\partial H}{\partial\mathbf{k}}, \tag{5}$$

where the scaling factor $C(\mathbf{x},\mathbf{k})=-(\partial H/\partial\omega)^{-1}$ is the same for all six partial derivatives. Therefore, $\{\partial H/\partial\mathbf{x},\partial H/\partial\mathbf{k}\}$ and $\{\partial\omega/\partial\mathbf{x},\partial\omega/\partial\mathbf{k}\}$ always point in the same direction. Thus Eq. (4) can also be written as

$$\frac{d\mathbf{r}}{dt}=\frac{\partial\omega(\mathbf{x},\mathbf{k})}{\partial\mathbf{k}},\quad \frac{d\mathbf{q}}{dt}=-\frac{\partial\omega(\mathbf{x},\mathbf{k})}{\partial\mathbf{x}}. \tag{6}$$

.

The curve $\{\mathbf{r}(t),\mathbf{q}(t)\}$ describes the same curve as $\{\mathbf{r}(\tau),\mathbf{q}(\tau)\}$, but parametrized by the parameter t instead of τ. Using the definition of group velocity $V_g=\partial\omega/\partial k$, $d\mathbf{X}/dt$ can now be identified with the group velocity, t can be identified simply as time, and $\mathbf{r}(t)$, $\mathbf{q}(t)$ can be identified with the optical ray path and the wave vector along the ray path, respectively.

Because the Hamiltonian equation, (4) is satisfied for either the $H(\mathbf{x},\mathbf{k})$ obtained in Eq. (3) or the dispersion relation $\omega(\mathbf{x},\mathbf{k})$, we will refer to both quantities as the Hamiltonian. We will consistently use $H(\mathbf{x},\mathbf{k})$ in the rest of the paper to denote the Hamiltonian. This notation signifies the equivalence of Eq. (4) to classical Hamiltonian equations in mechanics.

If we know $H(\mathbf{x},\mathbf{k})$ or the dispersion relation at each location in the bulk dielectric medium, then Eq. (4) can be integrated to give the ray path for all later times given the initial ray location, and the initial wave vector. For Eq. (4) to be valid, L needs to be large compared to the wavelength λ.

It should be noted that the Hamiltonian equations in optics are analogous to the WKB method of quantum mechanics. Both methods start by assuming a field that has an amplitude that varies much slower than the phase, and that scattering can be neglected. Useful approximations of the field pattern are then found by substituting into either Maxwell's equations or the Schrödinger equation as appropriate.

We will show in Sec. III that, if a packet of Bloch waves has a Gaussian distribution of the transverse $\mathbf{k}$ vector, the envelope of the field will behave like a Gaussian beam field. Therefore, by using the photonic crystal dispersion surface instead of the bulk medium dispersion surface, and Bloch waves instead of the plane wave components in a Gaussian beam, we can apply Eq. (4) to ray propagation in nonuniform photonic crystals. The same argument applies to the extended Hamiltonian equations, which we will develop next, in part B of this section. For clarity, we will introduce the extended Hamiltonian equations for Gaussian beam propagation in

bulk nonuniform dielectric media, keeping in mind that application to photonic crystals is straightforward.

B. Extension to beam width calculations

First we introduce some notations. We define a generalized coordinate system $\{\tau(\mathbf{x}), w^1(\mathbf{x})\ w^2(\mathbf{x})\}$ that is attached to the ray path R. The ray path R is given by the coordinate curve (τ, $w^1=0$, $w^2=0$). For the derivation of the extended Hamiltonian equations, we do not need an explicit expression for the mapping from the Cartesian system (x^1,x^2,x^3) to $\{\tau,w^1,w^2\}$. But we assume that, in the proximity of the ray path, the mapping from (x^1,x^2,x^3) to $\{\tau,w^1,w^2\}$ is unitary.

To simplify notation, we will use the subscripts to denote first and second partial derivatives with respect to x^α, e.g.,

$$f_\alpha \equiv \frac{\partial f}{\partial x^\alpha}, \quad g_\alpha \equiv \frac{\partial g}{\partial x^\alpha}, \quad g_{\beta\alpha} \equiv \frac{\partial g_\alpha}{\partial x^\beta}. \tag{7}$$

When we treat g as dependent on $\mathbf{x}$, we will use the symbol ∂_α to denote the partial derivative with respect to x^α, e.g.,

$$\partial_\alpha f(\nabla g(\mathbf{x}),\mathbf{x}) = \frac{\partial f}{\partial x^\alpha} + \frac{\partial f}{\partial g_\beta} g_{\beta\alpha}. \tag{8}$$

In Eq. (8) and all subsequent equations, Einstein's summation convention is adopted. That is, if an index occurs more than once in a product of terms, such as the index β above, summation over all values of the index is implied.

When we change coordinates to $\{\tau,w^1,w^2\}$, we will use the symbol ∂_i to denote the partial derivative with respect to w^i:

$$\partial_i f(\nabla g(\tau,w^1,w^2),(\tau,w^1,w^2)) = \frac{\partial f}{\partial w^i} + \frac{\partial f}{\partial g_\beta} g_{i\beta}. \tag{9}$$

∂_{ij} will similarly be the second derivative with respect to w^i and w^j.

We now extend the Hamiltonian optics method with equations for obtaining the beam width and the radius of curvature in periodic structures with slowly varying nonuniformities. To the best of our knowledge, beam width equations have not previously been applied to the analysis of periodic nanostructures with nonuniformities. We follow the extension of Hamiltonian optics developed by Poli *et al.* in Ref. [10] for plasmas. Assume again the nonuniformity is caused by a slowly varying dielectric tensor $\boldsymbol{\varepsilon}(\mathbf{x})$. Under the assumption that L is much greater than the wavelength λ, a Gaussian beam traveling in nonuniform media should resemble a Gaussian beam whose center is following some path. Therefore, we assume the field has the form

$$\mathbf{E}(\mathbf{x}) = \mathbf{a}(\mathbf{x})\exp[-\phi'(\mathbf{x}) + is'(\mathbf{x})] = \mathbf{a}(\mathbf{x})\exp[-ig'(\mathbf{x})], \tag{10}$$

where $\mathbf{a}(\mathbf{x})$ is the amplitude of the beam, $s'(\mathbf{x})$ is the phase of the beam, $\exp[-\phi'(\mathbf{x})]$ describes a Gaussian profile perpendicular to a central ray path, and $g'=s'+i\phi'$ defines a complex phase for this problem. Since we assume a Gaussian transverse beam profile, we have, in the coordinate system $\{\tau,w^1,w^2\}$:

$$\exp[-\phi'(\mathbf{x})] = \exp\left(-\tfrac{1}{2}\rho'_{ij}(\tau)w^i w^j\right), \tag{11}$$

where ρ'_{ij} specifies the beam width.

It is important to estimate and then keep track the relative rates of variation for the terms in Eq. (10). The medium property changes by a significant percentage over a distance of 1 unit (remember the coordinate system is scaled by L). Therefore we expect $\mathbf{a}(\mathbf{x})$ should also change by $O(1)$ (i.e., of order unity) over unit length. We can express this assumption as

$$\frac{|\nabla \mathbf{a}|}{|\mathbf{a}|} = O(1). \tag{12}$$

The optical phase s', on the other hand, should change by $O(2\pi L/\lambda)$ over unit length. Furthermore, we expect the beam picture to be valid when, perpendicular to the ray path, ϕ' causes the field to decay on a distance much shorter than L, but longer than λ. In the interest of keeping track of the relative sizes of the terms for later approximations in the derivation, we scale the terms in Eqs. (10) and (11):

$$\kappa = \frac{\omega L}{c} \gg 1,$$

$$s = \frac{1}{\kappa} s',$$

$$\rho_{ij} = \frac{1}{\kappa}\rho'_{ij}, \quad \phi = \frac{1}{\kappa}\phi',$$

$$g = s + i\phi = \frac{1}{\kappa} g'. \tag{13}$$

After the scaling, we will assume that $s(\mathbf{x})$, $\rho_{ij}(\mathbf{x})$ are of order the same size as $\mathbf{a}(\mathbf{x})$, and $s(\mathbf{x})$, $\phi(\mathbf{x})$, $\rho_{ij}(\mathbf{x})$ vary at of order the same rate as $\mathbf{a}(\mathbf{x})$. The ansatz for the field becomes

$$\mathbf{E}(\mathbf{x}) = \mathbf{a}(\mathbf{x})\exp(-\kappa\phi + i\kappa s) = \mathbf{a}(\mathbf{x})\exp(-i\kappa g). \tag{14}$$

By substituting the assumed form of $\mathbf{E}(\mathbf{x})$ into Maxwell's equation, and keeping only the terms on the order of κ^2, a matrix equation for $\mathbf{a}(\mathbf{x})$ can be obtained:

$$\left[\left(\frac{c}{\omega}\right)^2 (|\nabla g|^2 I - \nabla g \nabla g^T) - \boldsymbol{\varepsilon}(\mathbf{x})\right]\mathbf{a} \equiv \mathbf{P}\mathbf{a} = \mathbf{0}, \tag{15}$$

which gives our definition of the 3×3 matrix $\mathbf{P}(\nabla g,\mathbf{x})$. In order for a nontrivial solution to exist, we must have

$$\tilde{H}(\nabla g,\mathbf{x}) \equiv \det[\mathbf{P}(\nabla g,\mathbf{x})] = 0, \tag{16}$$

where we have introduced a "complex Hamiltonian" $\tilde{H}$. Note $\det[\mathbf{P}]=0$ is just Eq. (3) with $\mathbf{k}$ replaced by ∇g. Along R, $\phi=0$, and $\tilde{H}$ reduces to the real Hamiltonian H given in Eq. (2). Therefore, Eq. (16) is satisfied along R. We seek a solution to Eq. (16) in the neighborhood of R, when $\phi\neq 0$. By expanding Eq. (15) in w^1, w^2 around R, and keeping track of the size of the terms, it can be shown that Eq. (16) is satisfied to sufficient accuracy in the neighborhood of R if the following expressions hold [10]:

$$\tilde{H}|_R = 0, \tag{17a}$$

$$\partial_i \tilde{H}|_R = 0, \tag{17b}$$

$$\partial_{ij} \tilde{H}|_R = 0. \tag{17c}$$

Because of Eq. (17a), and the fact that τ is measured along R, all derivatives of $\tilde{H}$ with respect to τ are zero. We can now rewrite these expressions in the coordinate system (x^1, x^2, x^3):

$$\begin{aligned}\partial_\alpha \tilde{H}|_R &= w^i_\alpha \partial_i \tilde{H} + \tau_\alpha \left.\frac{\partial \tilde{H}}{\partial \tau}\right|_R \\ &= w^i \partial_i \tilde{H}|_R + \tau_\alpha \frac{\partial}{\partial \tau}(\tilde{H}|_R) \\ &= w^i_\alpha \partial_i \tilde{H}|_R. \end{aligned} \tag{18}$$

Similarly, taking one more derivative,

$$\partial_{\alpha\beta} \tilde{H}|_R = w^i_\alpha w^j_\alpha \left.\frac{\partial^2 \tilde{H}}{\partial w^i \partial w^j}\right|_R. \tag{19}$$

Using Eq. (17) in Eqs. (18) and (19) , we have

$$\tilde{H}|_R = 0, \tag{20a}$$

$$\partial_\alpha \tilde{H}|_R = 0, \tag{20b}$$

$$\partial_{\alpha\beta} \tilde{H}|_R = 0. \tag{20c}$$

This statement is trivial if we replace $\tilde{H}$ with the real Hamiltonian H. But, here we are claiming that the imaginary part of $\tilde{H}$ also has a zero second derivative along R. Expansion of Eq. (20) using Eq. (8) will give the equations governing the evolution of the beam width along R.

We can expand Eq. (20c) by applying Eq. (8) twice. Because $\tilde{H}$ is equal to the real Hamiltonian H along R, and $\phi(\mathbf{x})$ has zero first derivative along R, we can simplify the expansion to the following expression. The expression involves only derivatives of the real Hamiltonian H with respect to the real part of the phase:

$$\begin{aligned}\partial_{\alpha\beta} H|_R &= \partial_\beta \left(\frac{\partial \tilde{H}}{\partial x^\alpha} + \frac{\partial \tilde{H}}{\partial g_\gamma} g_{\gamma\alpha} \right) = \frac{\partial^2 H}{\partial x^\alpha \partial x^\beta} + \frac{\partial^2 H}{\partial x^\alpha \partial s_\delta} g_{\delta\beta} \\ &\quad + \frac{\partial^2 H}{\partial s_\gamma \partial x^\beta} g_{\gamma\alpha} + \frac{\partial^2 H}{\partial s_\gamma \partial s_\delta} g_{\gamma\alpha} g_{\delta\beta} + \frac{\partial H}{\partial s_\gamma} g_{\gamma\alpha\beta} \\ &= \frac{\partial^2 H}{\partial x^\alpha \partial x^\beta} + \frac{\partial^2 H}{\partial x^\alpha \partial s_\delta} g_{\delta\beta} + \frac{\partial^2 H}{\partial s_\gamma \partial x^\beta} g_{\gamma\alpha} \\ &\quad + \frac{\partial^2 H}{\partial s_\gamma \partial s_\delta} g_{\gamma\alpha} g_{\delta\beta} + \frac{dg_{\alpha\beta}}{d\tau} \\ &= 0. \end{aligned} \tag{21}$$

In the third step above we used the original Hamiltonian equation to write

$$\frac{dg_{\alpha\beta}}{d\tau} = g_{\alpha\beta\gamma} \frac{dx^\gamma}{d\tau} = g_{\alpha\beta\gamma} \frac{\partial H}{\partial s_\gamma}. \tag{22}$$

Equation (21) is a system of ordinary differential equations governing the evolution of $g_{\alpha\beta}$ along the ray path R. We will write the real and imaginary parts separately, and refer to these equations as the system of extended Hamiltonian equations

$$\begin{aligned}\frac{ds_{\alpha\beta}}{d\tau} &= -\frac{\partial^2 H}{\partial x_\alpha \partial x_\beta} - \frac{\partial^2 H}{\partial x_\beta \partial k_\gamma} s_{\alpha\gamma} - \frac{\partial^2 H}{\partial x_\alpha \partial k_\gamma} s_{\beta\gamma} \\ &\quad - \frac{\partial^2 H}{\partial k_\gamma \partial k_\delta} s_{\alpha\gamma} s_{\beta\delta} + \frac{\partial^2 H}{\partial k_\gamma \partial k_\delta} \phi_{\alpha\gamma} \phi_{\beta\delta}, \\ \frac{d\phi_{\alpha\beta}}{d\tau} &= -\left(\frac{\partial^2 H}{\partial x_\alpha \partial k_\gamma} + \frac{\partial^2 H}{\partial k_\gamma \partial k_\delta} s_{\alpha\delta} \right) \phi_{\beta\gamma} \\ &\quad - \left(\frac{\partial^2 H}{\partial x_\beta \partial k_\gamma} + \frac{\partial^2 H}{\partial k_\gamma \partial k_\delta} s_{\beta\delta} \right) \phi_{\alpha\gamma}. \end{aligned} \tag{23}$$

Note the physical significance of the equations. The second derivative of $\phi(\boldsymbol{x})$ will give the beam width measured along each spatial coordinate. The second derivative of $s(\boldsymbol{x})$ gives the radius of curvature of the phase fronts along each spatial coordinate

$$s_{\alpha\alpha} = \frac{\omega}{cR_\alpha}, \quad \phi_{\alpha\alpha} = \frac{2}{W_\alpha^2}. \tag{24}$$

The beam width is then given by

$$W(\tau) = \frac{W_x W_y}{\sqrt{W_x^2 + W_y^2}}. \tag{25}$$

Here we used the definition of the beam width as the distance from the center of the beam where the field amplitude has fallen to $1/e$ of the maximum.

Equation (23) is exact for a beam propagating in homogenous medium, and a good approximation in an inhomogeneous medium when $L/W \gg 1$, where L is the characteristic inhomogeneity length. For homogenous media, Eq. (23) reduces to equations for the beam width and the radius of curvature of a freely propagating Gaussian beam. As we discuss in the next section, for a periodic medium with nonuniformity, Eq. (23) still describes the beam width, and can be easily integrated numerically since it is a system of linear ordinary differential equations.

III. GAUSSIAN BEAM IN A LOCALLY PERIODIC MEDIUM

In the discussion above of the extended Hamiltonian equations, we introduced the Hamiltonian equations and the extended Hamiltonian equations in the context of Gaussian beams propagating in slowly varying, anisotropic, bulk media. The application to slowly varying, locally periodic media, in which the properties of the unit cell change slowly from cell to cell, is straightforward by using the Bloch wave dispersion relation instead of the Hamiltonian for bulk me-

dia. Eigenstates in a periodic medium for a given wave vector $\mathbf{k}$ can be written in the Bloch form

$$\boldsymbol{\psi}_{\mathbf{k}} = e^{j\mathbf{k}\cdot\mathbf{x}}\mathbf{u}_{\mathbf{k}}(\mathbf{x}), \tag{26}$$

where $\boldsymbol{\psi}_{\mathbf{k}}$ is either the E field or the H field, $\mathbf{u}_{\mathbf{k}}(\mathbf{x})$ is a periodic function with the same period as the lattice, and $\mathbf{x}$ is the position. The dispersion relation $\omega(\mathbf{k})$ for the Bloch wave can be obtained using various methods. For such periodic media, the dispersion relation corresponds to a band structure, very similar to the band structures found for the Schrödinger equation for electrons in a periodic lattice, and the calculation of such band structures is a core part of the study of periodic optical media (i.e., photonic crystals). A key point about the present work is that, if we have calculated that band structure or dispersion relation for each different possible locally periodic region, we may take all the results considered above for slowly varying bulk media, and apply those now to the case of media that are locally periodic. We merely have to substitute the local dispersion relation of the locally periodic medium for the local dispersion relation of the material in the bulk case; no other change is necessary for analyzing the propagation in locally periodic media, at least within the approximations of the method.

We still need to show that, when a Gaussian beam traveling in free space enters a periodic medium, the transmitted wave form inside the periodic medium can still be described by a Gaussian beam equation. A solution of the scalar wave equation can be written in its plane wave components

$$\boldsymbol{\psi}_{\text{bulk}}(\mathbf{x}) = \frac{1}{2\pi}\int_{-\infty}^{\infty}\int_{-\infty}^{\infty} A(k_x,k_y)\exp[j\mathbf{k}\cdot\mathbf{x}]dk_x dk_y, \tag{27}$$

where $\mathrm{k}=\{k_x,k_y,k_z\}$ is the wave vector and $A(k_\mathrm{x},k_\mathrm{y})$ is the amplitude of the plane wave components. A Gaussian beam can be described by a field in this form. If we assume the Gaussian beam travels along the z axis, it is possible to find a equation for $A(k_\mathrm{x},k_\mathrm{y})$:

$$A(k_x,k_y) = \frac{1}{\sqrt{\pi W^2}}\exp\left[-\frac{W^2}{4}(k_x+k_y)^2\right], \tag{28}$$

where W is the beam width. If the W is large, A decays to negligible values when $k_\perp$ approaches $|\mathbf{k}|$. In other words, the plane wave components only span a small angle in k space. Equation (28) is only valid in the paraxial approximation

$$k_z \approx k - \frac{k_x^2+k_y^2}{2k}, \tag{29}$$

where $k=(k_\mathrm{x}^2+k_\mathrm{y}^2+k_\mathrm{z}^2)^{1/2}$ is the magnitude of the wave vector. In particular, in order for the plane waves described by Eq. (29) to combine as to a Gaussian beam, we must use the paraxial approximation to express k_z in Eq. (27) as a quadratic function of k_x and k_y [11]:

$$\boldsymbol{\psi}_{\text{bulk}}(\mathbf{x}) = \frac{1}{2\pi}\int_{-\infty}^{\infty}\int_{-\infty}^{\infty} A(k_x,k_y)\exp\left[jk_x x + jk_y y + j\left(k - \frac{k_x^2+k_y^2}{2k}\right)z\right]dk_x dk_y. \tag{30}$$

After expressing the incident Gaussian beam in its plane wave components, we can see how these components transform when they enter the periodic medium.

When a Gaussian beam traveling in a bulk medium impinges on a periodic medium, phase matching requires that each incident plane wave component only transfers energy to the Bloch wave with the same transverse wave vector component k_x and k_y (assuming the wave vectors are concentrated in the first Brillouin zone):

$$\boldsymbol{\psi}_{pc}(\mathbf{r}) = \frac{1}{2\pi}\int_{-\infty}^{\infty}\int_{-\infty}^{\infty} T(k_x,k_y)A(k_x,k_y)\boldsymbol{\psi}_{\mathbf{k}}dk_x dk_y, \tag{31}$$

when $T(k_\mathrm{x},k_\mathrm{x})$ is the transmission coefficient from a plane wave to its corresponding Bloch wave and $A(k_\mathrm{x},k_\mathrm{y})$ is given by Eq. (28). If the incident beam is wide, then k_x, k_y spans a small range, and we can assume that the transmission coefficient T is not a function of k_x, k_y. We can then express the field inside the periodic medium as

$$\begin{aligned}\boldsymbol{\psi}_{pc}(\mathbf{r}) &= \frac{1}{2\pi}T\int_{-\infty}^{\infty}\int_{-\infty}^{\infty} A(k_x,k_y)\boldsymbol{\psi}_{\mathbf{k}}dk_x dk_y \\ &= \frac{1}{2\pi}\mathbf{u}(\mathbf{r})T\int_{-\infty}^{\infty}\int_{-\infty}^{\infty} A(k_x,k_y)e^{j\mathbf{k}\cdot\mathbf{x}}dk_x dk_y.\end{aligned} \tag{32}$$

In the last step above, we assumed $\mathbf{u}_{\mathbf{k}}(\mathbf{r})$ is constant independent of $\mathbf{k}$, again because the Gaussian beam spans a small angle in k space. In order for the integral term to match the equation for a Gaussian beam, we need to be able to express k_z as a quadratic function of k_x and k_y as in Eq. (30). From the Bloch wave dispersion relation $\omega(\mathbf{k})=\omega_0$, we can find k_z in the form $k_\mathrm{z}=f(k,k_\mathrm{x},k_\mathrm{y})$, which is not in general in the form $k_\mathrm{z}=(k^2-k_\mathrm{x}^2-k_\mathrm{y}^2)^{1/2}$. But, if the angular spread of k is small, we can always approximate $f(k,k_\mathrm{x},k_\mathrm{y})$ around the average k vector $(k_{\mathrm{x}0},k_{\mathrm{y}0},k_{\mathrm{z}0})$ as

$$\begin{aligned}f(k,k_x,k_y) \approx k_{z0} &+ \sum_{\alpha=x,y}\frac{\partial f}{\partial k_\alpha}(k_\alpha - k_{\alpha 0}) \\ &+ \frac{1}{2}\sum_{\beta=x,y}\sum_{\alpha=x,y}\frac{\partial^2 f}{\partial k_\alpha \partial k_\beta}(k_\alpha - k_{\alpha 0})(k_\beta - k_{\beta 0}).\end{aligned} \tag{33}$$

Using this approximation in Eq. (32), we can express k_z as a quadratic function of k_x and k_y as in Eq. (30). Except for the addition of terms linear in k_x and k_y, the integral term in Eq. (32) then corresponds exactly with the equation of a Gaussian beam. Just as in an anisotropic medium, the linear terms corresponds to changes in beam propagation angle, which does not alter the Gaussian beam shape. This shows that, when the incident Gaussian beam is wide, the envelope of $\boldsymbol{\Psi}_{pc}$ behaves as a Gaussian beam. Therefore, we can use the extended Hamiltonian equations developed for the bulk me-

dium directly for a locally periodic medium, simply by replacing the bulk medium dispersion relation $\omega(\mathbf{k})=f(H_{\text{bulk}})$ with the Bloch wave dispersion relation.

IV. VALIDITY OF THE EXTENDED HAMILTONIAN EQUATIONS

A. Measure of validity

In Eq. (14), we made an assumption on the relative sizes and the relative rates of change of the terms, and tracked the order of the corresponding approximations through the parameter $\boldsymbol{\kappa}$. Recall that the parameter $\boldsymbol{\kappa}=L/\lambda \gg 1$ describes the fact that the structure varies slowly over many wavelengths of the field. It can be shown that the assumed orders of the terms in Eq. (14) are equivalent to the following statement on the comparison of orders of terms:

$$W/\lambda \sim L/W \sim \boldsymbol{\kappa}^{1/2} \gg 1, \tag{34}$$

where W is the beam width. In other words, in the derivation of the extended Hamiltonian equations, starting with Eq. (14), we assumed that the beam width is much larger than the wavelength, and the medium inhomogeneity length is much larger than the beam width. The extended Hamiltonian equations are only valid when $\boldsymbol{\kappa}^{1/2}$ is much greater than 1.

We have not quantitatively defined the characteristic inhomogeneity length L, which is needed if we would like to evaluate the validity of the extended Hamiltonian equations. In deriving the extended Hamiltonian equations, we specified that the field amplitude $\mathbf{a}(\mathbf{x})$ varied significantly over L [Eq. (12)]. In order for $\mathbf{a}(\mathbf{x})$ to change at the rate given by Eq. (12), the determinant of the matrix multiplying $\mathbf{a}(\mathbf{x})$ in Eq (1), i.e., H, must change at the same rate. Therefore L can be estimated as

$$L = \min_{\mathbf{x}} \frac{H(\mathbf{k},\mathbf{X})}{|\nabla H(\mathbf{k},\mathbf{X})|}, \tag{35}$$

where the spatial divergence $\nabla H(\mathbf{k},\mathbf{x})$ is taken with $\mathbf{k}$ as a independent variable and evaluated in the real spatial coordinate system $\{\mathbf{X}\}$ rather than the normalized coordinate system $\{\mathbf{x}\}$. The validity of the extended Hamiltonian equations can be checked by finding L using Eq. (35) and comparing it to W and λ. For example, if the wavelength is 1.5 μm, the structure should vary slowly over several hundreds of μm in order to have $\boldsymbol{\kappa}^{1/2}$ much greater than 1.

B. Comparison with FDTD

We can verify the validity of the proposed extended Hamiltonian method with a specific FDTD simulation. The basic structure is a 120 by 120 square lattice of high index rods ($n=2.54$) in a low index background ($n=1.56$). The rod radius $\rho(\boldsymbol{x})$ is varied as a hyperbolic function in the spatial coordinates $\rho(\boldsymbol{x})=\alpha(x^2+y^2)+\rho_0$, where $\rho_0=0.28$, $\alpha=8\times10^{-6}$, and x,y are measured in lattice constants a. We set the frequency to be $\omega=0.28(2\pi c/a)$. A Gaussian beam with a flat phase front enters the structure near the upper left hand corner. The beam width W as defined in Eq. (23) is set to 12 lattice constants, and the incident phase front is perpendicular to the structure boundary. We consider only the TM polarization, that is, the E field points out of the plane of the 2D periodicity. A 2-D FDTD method with perfectly matched layer boundary conditions [12] is used in the simulation.

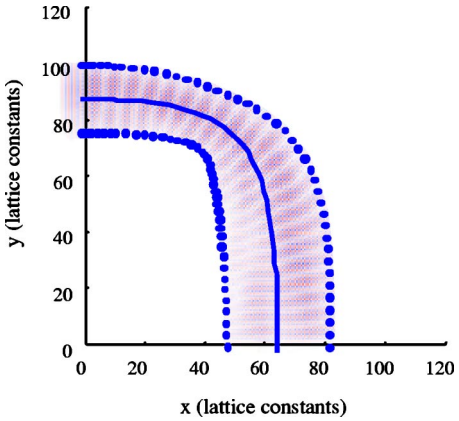

FIG. 1. (Color online) Comparison of the extended Hamiltonian method with FDTD simulation. The center dotted line is the beam path, the dots on each side show the beam width calculated using Eq. (23). The underlying shading shows the intensity of the E field from FDTD.

The instantaneous field in steady state is plotted in Fig. 1. The hyperbolic variation of the rod radius causes the beam to bend and exit on the bottom boundary of the 120×120 lattice. The fine structure of the field is strongly affected by the periodicity of the medium, and can be attributed to the periodic term in the Bloch waves (see Sec. III). Because the input beam is fairly wide, the envelope of the field approximates a Gaussian beam as predicted in Sec. III.

Some features of the Gaussian beam envelope can be attributed to phenomena known in bulk optics. For example, even though the input beam has a flat phase front, the beams narrows halfway into the structure. This is due to the hyperbolic distribution of the nonuniformity, which acts as a lens. The lensing effect is opposed by the diffraction of the beam, which dominates before the beam exits the structure and the beam widens.

The beam path and beam width calculated with Eqs. (4) and (23) are plotted over the FDTD simulation results in Fig. 1. The two methods are in good agreement. In particular, the extended Hamiltonian method is successful in predicting the lensing effect of the nonuniformity. This is accomplished by the terms in Eq. (23) that involve partial derivatives of the dispersion relation H with respect to spatial coordinates. The partial derivatives of the dispersion relation H with respect to k-space coordinates describe all diffraction effects. By accounting for both diffraction and spatial lensing, Eq. (23) gives the beam width in quantitative agreement with FDTD, but with significantly less computional cost. The FDTD simulation took 2 days to run on a Sun SPARC Ultra-4 workstation.

The Hamiltonian method does require preliminary calculations to evaluate the dispersion relation for each possible unit cell structure. Here, we calculated the dispersion relation $\omega(\mathbf{k})$ for 50 rod radius values spaced evenly from $0.1a$ to $0.5a$ (where a is the lattice constant), and used sixth order

polynomials to interpolate between the rod radius values for each **k**. This calculation took 1 day to run on the same workstation. Having performed these preliminary calculations, the subsequent calculation for any specific nonuniform structure is very rapid. For the structure in Fig. 1, the extended Hamiltonian equations were solved in 2 s in a poorly optimized Matlab code on a similar workstation.

The extended Hamiltonian method has its limitations. The situation we have chosen to model here is deliberately extreme, and pushes the limits of validity of the approximations underlying the Hamiltonian approach. In the FDTD result shown in Fig. 1, the transverse beam profile is deviating from a Gaussian profile. Equation (23) cannot model any deviation from a Gaussian profile, because the beam width calculation only uses the second order derivative of the nonuniformity along the beam path. The slight breakup of the beam can be attributed to the magnitude of the nonuniformity of this structure. As defined in the Sec. IV, the characteristic inhomogeneity length L for this structure is around 100 lattice constants, while the beam width reaches 20 lattice constants at places. This challenges the slowly varying approximation, which requires $\kappa^{1/2}=L/W\gg 1$. It may be possible to include higher order terms to increase the tolerance of the extended Hamiltonian method to large nonuniformities. This is left as a topic for future research.

C. Comparison with tracing ray bundles

Another method for tracking the evolution of an electromagnetic field through an inhomogeneous medium is by tracing a family of rays. Decomposing an initial transverse field distribution into its plane-wave components, we get an initial k-vector distribution. For example, we see that the Gaussian field is composed of planewaves with a Gaussian distribution in the transverse k vector [Eq. (28)]. We can define a set of rays with an initial transverse k-vector distribution matching the initial k-vector distribution. Then, each ray in this set can be traced independently, using the conventional Hamiltonian equations [Eq. (4)]. It can be shown that, away from where the rays intersect, i.e., the caustic points, properties of the field can be approximated well by the ray family. Furthermore, it can be shown that even near caustic points such as the beam waist, the field can be reconstructed from the ray family by associating a Gaussian field contribution to each ray and summing over the ray family [13]. Because tracing a ray family solves a set of ordinary differential equations (ODEs) that takes into consideration of the medium nonuniformity over many ray paths, it can be used to highlight and explain the limitations of the extended Hamiltonian method.

Figure 2 shows the ray paths for a family of rays through the same structure explained in Sec. V. If the input beam is Gaussian with $W=12a$, then the initial transverse k-vector distribution (in unit of $2\pi/a$) is Gaussian with a width of $1/2W=1/24a$. The ray family traced in Fig. 2 has a k-vector distribution that is angularly evenly spaced, with transverse k spanning $(-1/24a,\ 1/24a)$. The spacing between the rays, away from the caustic points, becomes a function of the intensity of the field. At the exit plane of the structure in Fig. 2,

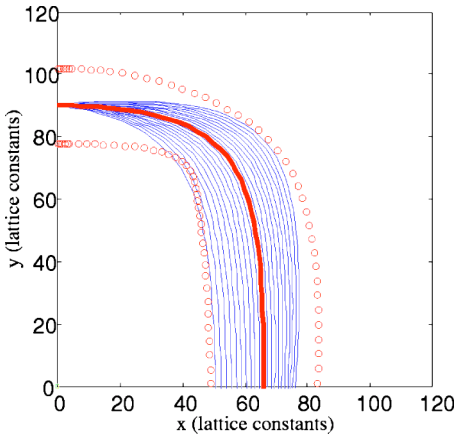

FIG. 2. (Color online) Comparison of the extended Hamiltonian method with ray family tracing. The thick solid line is the reference ray path. Thinner lines are the ray paths with initial transverse k spanning $(-1/24a,\ 1/24a)$. Circles illustrate the width of the beam calculated with the extended Hamiltonian equations.

the spacing between the rays becomes skewed, with a higher concentration of the rays on the right hand side of the beam center. This matches well with the FDTD simulation in the previous section. The skewed field originates from the highly skewed nonuniformity relative to the beam center. The extended Hamiltonian method does not model the beam skewing, because the extended Hamiltonian equations only depend on the medium property (the second derivatives of H) along the beam center. Each ray in the ray family, on the other hand, probes parts of the structure away from the beam center, and therefore models the effect of the skew.

Compared to the extended Hamiltonian method, a set of ODE's needs to be solved for tracing the ray bundle, one for each ray. This greatly increases the computational cost. Also, compared to tracing a ray bundle, if the transverse field is approximately Gaussian, it is much easier to use the extended Hamiltonian method [through Eq. (23)] to estimate the beam width and the radius of curvature. Nevertheless, tracing the ray bundle is a viable tool for checking the results of the extended Hamiltonian method. For extreme structures, tracing the ray bundle helps to assess of breakdown of the extended Hamiltonian method.

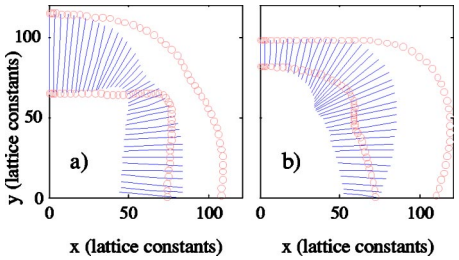

FIG. 3. (Color online) Effect of input beam width on output beam separation. Calculated using the extended Hamiltonian method. The dotted curves denote the beam width at $\omega=0.28(2\pi c/a)$. The fence line shows the beam width at $\omega=0.285(2\pi c/a)$. (a) Wide input beams will cause the output beams to overlap. (b) If input beams are too narrow, diffraction dominates and output beams still overlap.

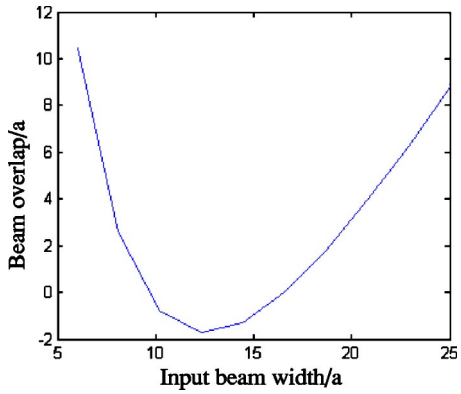

FIG. 4. (Color online) Dependency of output beam overlap on input beam width. a=lattice constant.

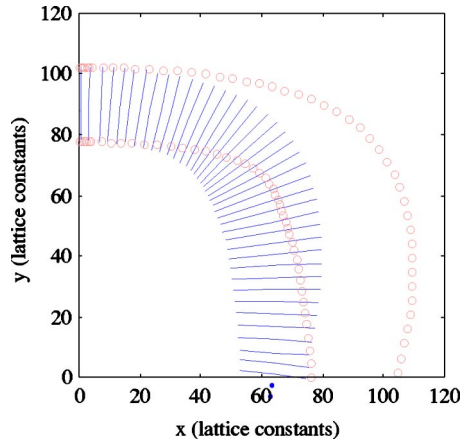

FIG. 5. (Color online) Beam profile with optimal input beam width. The dotted curves outline the beam width at $\omega=0.28$. The fence line shows the beam width at $\omega=0.285$.

V. NUMERICAL OPTIMIZATION

The extended Hamiltonian method is not only an analysis tool similar to FDTD. The low computational cost of the method, once the underlying dispersion relations have been calculated for the range of unit cells of interest, enables the design and optimization of the photonic crystal nonuniformity for device functions. We demonstrate this with an example of optimizing the beam width separation. The basic structure is the same as in the FDTD experiment, with the same rod radius distribution $\rho(\boldsymbol{x})=(x^2+y^2)+\rho_0$. For a fixed rod radius distribution, the exit beam location on the bottom boundary depends on the frequency, and the exit beam width depends on both the frequency and the beam width at the input. In this example, we would like to maximize the separation of two beams at $\omega=0.28(2\pi c/a)$ and $0.285(2\pi c/a)$ by optimizing the input beam width. It is possible to optimize more properties of the device simultaneously, such as the parameters of the hyperbolic function and the input beam. But this single parameter optimization example is sufficient to demonstrate the use of the extended Hamiltonian equations to design desired functions.

An optimal input beam width exists. As the input beam width approaches zero the output beam width approaches infinity due to diffraction; if, conversely, the input beam width is very large, then the output beam width will also be large (Fig. 3). Intuitively, in order to maximize the beam separation for $\omega=0.28(2\pi c/a)$ and $0.285(2\pi c/a)$, the input beam width should be chosen so that the Rayleigh length is close to the beam path lengths in the device. Because two frequencies are involved, and the structure is nonuniform, numerical optimization is needed to find the optimal beam width quantitatively. Such an optimization requires repeated calculation of the exit beam width, which is practically impossible by FDTD but straightforward by the extended Hamiltonian method.

Assuming the two beams exit the structure at $y=0$ at locations x_1 and x_2, we define the overlap of the two beams as $(x_2-x_1)-(W_1+W_2)$, where W_1 and W_2 are the widths of the beams. Figure 4 shows the exit beam overlap as a function of the input beam width. For each input beam width, the extended Hamiltonian equations were used to calculate the beam width and beam location at the output for each frequency. The maximum beam separation occurs when the input beam half width is around 12.5 lattice constants. Figure 5 shows the beam profiles with the optimal input beam width. The output beams from the two different frequencies are separated by two lattice constants at their $1/e^2$ intensity points. The nonuniformity makes it difficult to find analytical solutions for the optimal beam width. This illustrates the importance of numerical optimization even for such relatively simple structures. Without an analysis method much faster than FDTD, design by numerical optimization would have been impossible.

VI. CONCLUSION

We have introduced a set of equations for tracking the beam width in periodic nanostructures with nonuniformities, and confirmed the validity of the equations with FDTD simulations. We have demonstrated the use of the extended Hamiltonian method to design a frequency demultiplexing device and optimize the beam separation. We believe this extension will supplement the Hamiltonian equations to enable more quantitative design and analysis of useful devices such as frequency demultiplexers, beam steering devices, and other photonic nanostructures, especially those deliberately exploiting non-uniform structures, without resorting to FDTD simulations.

ACKNOWLEDGMENTS

Y.J. gratefully acknowledges the support of the NSFGRF and NSF support under Grant No. ECS-02-00445.

[1] E. Yablonovitch, Phys. Rev. Lett. **58**,2059 (1987).
[2] S. John, Phys. Rev. Lett. **58**, 2486 (1987).
[3] J. D. Joannopoulos, R. D. Meade, and J. N. Winn, *Photonic Crystals: Molding the Flow of Light* (Princeton University Press, Princeton, NJ, 1995).
[4] N. Matuschek, F. X. Kartner, and U. Keller, IEEE J. Quantum Electron. **35**,129 (1999).
[5] M. Gerken and D. A. B. Miller, Appl. Opt. **42**,1330 (2003).
[6] A. Taflove and S. C. Hagness, *Computational Electrodynamics: The Finite-Difference Time-Domain Method*, 2nd. ed. (Artech House, Boston, 2000).
[7] P. Russell, J. Lightwave Technol. **17**, 1982 (1999).
[8] P. Wilkinson and M. Fromhold, Opt. Lett. **28**, 1034 (2003).
[9] J. A. Arnaud, *Beam and Fiber Optics* (Academic, New York, 1976).
[10] E. Poli, G. V. Pereverzev, and A. G. Peeters, Phys. Plasmas **6**, 5 (1999).
[11] H. A. Haus, *Waves and Fields in Optoelectronics* (Prentice Hall, New Jersey, 1984).
[12] J. P. Berenger, J. Comput. Phys. **114**, 185 (1994).
[13] G. W. Forbes and M. A. Alonso, J. Opt. Soc. Am. A **18**, 1132 (2001).